Quantitative structure-activity relationship for 4-hydroxy-2-alkenal induced cytotoxicity in L6 muscle cells*

Nicolas J. Pillon[1,2,3,4,5]*, Laurent Soulère[1,6], Roxane E. Vella[1,2,3,4,5], Marine Croze[1,2,3,4,5], Bertrand Caré[1,2,3,4,5], Hedi A. Soula[1,2,3,4,5], Alain Doutheau[1,6], Michel Lagarde[1,2,3,4,5] and Christophe O. Soulage[1,2,3,4,5]

*NOTICE: this is the author's version of a work that was accepted for publication in Chemico-Biological Interactions. Changes resulting from the publishing process, such as peer review, editing, corrections, structural formatting, and other quality control mechanisms may not be reflected in this document. Changes may have been made to this work since it was submitted for publication. A definitive version was subsequently published in Chemico-Biological Interactions 188 (2010) 171–180. DOI: 10.1016/j.cbi.2010.06.015

[1]Université de Lyon, F-69622, Lyon, France
[2]INSA-Lyon, RMND, F-69621, Villeurbanne, France
[3]INSERM U870, IMBL, F-69921, Oullins, France
[4]INRA U1235, Faculté Lyon Sud, F-69921, Oullins, France
[5]Hospices Civils de Lyon, Lyon, F-69003, France.
[6]ICBMS, CNRS UMR 5246, F-69622, Villeurbanne, France

***Corresponding author:**

Nicolas J. PILLON
RMND, Régulations Métaboliques Nutrition et Diabètes
Bâtiment IMBL,
INSA-Lyon, 20 avenue Albert EINSTEIN
69621 VILLEURBANNE cedex
FRANCE

Tel : +33 4 72 43 72 35
Fax : +33 4 72 43 85 24
E-mail : nicolas.pillon@insa-lyon.fr

Running title: Cytotoxicity of 4-hydroxy-2-alkenal derivatives

Word count: 4183

3 Tables, 5 Figures

ABSTRACT (299 words)

Lipid peroxidation is one of the most important sources of endogenous toxic metabolites. 4-hydroxy-2-nonenal (HNE) and 4-hydroxy-2-hexenal (HHE) are produced in several oxidative stress associated diseases from peroxidation of n-6 and n-3 polyunsaturated fatty acids, respectively. Both are able to form covalent adducts with many biomolecules. Particularly, proteins adduction can induce structural and conformational changes and impair biological function, which may be involved in the toxicity of hydroxyalkenals. The aim of this study was to compare the effect of 4-hydroxy-2-alkenals to several chemically related derivatives in order to clarify the physico-chemical requirement of their toxicity. L6 muscle cells were treated with HHE, HNE and parent derivatives (acetal derivative, trans alkenals and alkanals). Viability and necrosis were estimated using MTT, LDH and caspase-3 tests. $\log LC_{50}$ (Lethal Concentration 50) were then tested for correlation with adducts formation (estimated using dinitrophenylhydrazine) and several molecular descriptors in order to establish quantitative structure-toxicity relationship (QSTR) models. The rank of derivatives toxicity, based on IC_{50} was: hydroxy-alkenals > acetal derivatives ≈ 2-alkenals > alkanals and a high correlation was found between $\log IC_{50}$ and protein carbonylation. Moreover, $\log IC_{50}$ was correlated to the electrophilic descriptor LUMO (Lowest Unoccupied Molecular Orbital) as well as with electronegativity-related molecular descriptors such as number of oxygen atoms, partial negative surface area (PNSA3) and partial positive surface area (PPSA3). Together, these results point out the important role of the electrophilic structure and adduct formation in hydroxy-alkenals toxicity. Our present study demonstrates that 4-hydroxy-2-alkenals dramatic effects on cell viability are due to covalent adducts formation, particularly Michael adducts. This capacity is related to the electrophilic structure and reactive C=C double bond, making it highly accessible for nucleophilic addition. The present study suggests that nucleophilic scavengers might protect cells against electrophiles compounds and might be of possible therapeutic value in oxidative stress associated diseases.

Keywords: oxidative stress**,** lipid peroxidation, aldehydes, 4-hydroxy-2-nonenal, 4-hydroxy-2-hexenal, QSTR

1 Introduction

Endogenous reactive oxygen species (ROS) generated from aerobic metabolism play a key role in the pathogenesis of many types of diseases and tissue injuries. [1-4]. ROS are constantly produced within the body from normal oxidative metabolism, involving oxygen, oxidases and electron transport chain in mitochondrias. In pathological conditions, ROS production can dramatically increase, leading to the production of various damaging oxidation by-products. Lipid peroxidation is involved in the pathogenesis of numerous diseases including neurodegenerative diseases, atherosclerosis, diabetes, cancer, arthritis as well as in ethanol and drug-associated toxicity, postischaemic reoxygenation injury or aging process [5,6]. Due to the presence of carbon-carbon double bonds in unsaturated fatty acids residues, cell membranes phospholipids are particularly susceptible to ROS. Their oxidation leads to the production of lipid hydroperoxides and non-radical intermediates derived from unsaturated fatty acids. Lipid peroxidation generates a large amount of by-products such as 2-alkenals, 4-hydroxy-2-alkenals or ketoaldehydes [5]. These lipid aldehydes, considered as secondary peroxidation by-products, represent both markers of oxidative injury and toxic second messengers. These lipid peroxidation by-products are often more deleterious than ROS themselves as they can diffuse within the cells and tissues and thus propagate their noxious action [7].

Peroxidation of n-6 and n-3 polyunsaturated fatty acids leads to the production of several breakdown products, including 4-hydroxy-2-nonenal (HNE) and 4-hydroxy-2-hexenal (HHE), respectively [8-12]. Both moieties have been shown to be produced under oxidative stress conditions and to elicit cell death in many cell types. These 4-hydroxy-2-alkenals are able to induce apoptosis or necrosis [13-16], depending on cell types and concentrations used, and the mechanism of HNE-induced cell death has recently been pointed out. This includes activation of the caspase cascade, c-jun N-terminal (JNK) and p38 mitogen-activated protein kinases [17-19]. The toxicity of 4-hydroxy-2-alkenals is linked to their peculiar structures consisting of an aldehyde group with a conjugated double bond and a hydroxyl next to the unsaturation. This especially electrophilic structure is responsible for their great reactivity and ability to form adducts with many types of biomolecules such as reduced glutathione, proteins, lipids and DNA [20-22]. A Michael addition can occur through the reaction between the double bond of hydroxyalkenals and biomolecules containing amino and/or thiol groups (as in cysteinyl-containing molecules). On the other hand, Schiff bases can be formed by involvement of the carbonyl group and amino groups of biomolecules [23]. Adduction

on proteins, through structural and conformational changes, can impair their biological function and may be involved in the toxicity of hydroxyalkenals and potentially lead to cytotoxicity [24,25]. In addition, adduction on nucleotides in DNA can result in mutagenesis and altered gene expression [22,26].

As their peculiar chemical structure could be a major determinant of their toxicity, the aim of the present study was to compare the effect of 4-hydroxy-2-alkenals to several chemically related derivatives in order to establish a structure-toxicity relationship. Chemical groups involved in the formation of adducts were altered to test the involvement of each of them in 4-hydroxy-2-alkenal toxicity. Then, acetal derivatives, *trans*-2-alkenal and alkanals were used to achieve this purpose. Quantitative structure activity relationship (QSAR) or quantitative structure toxicity relationship (QSTR) models have become important tools to predict and understand the toxicity of chemical compounds. The aim of the present study was the development of QSTR models of toxicity for 4-hydroxy-2-alkenals in mammalian cultured cells. We therefore evaluated the physico-chemical requirement of hydroxyalkenal derivatives to exert cytotoxicity.

2 Material and methods

2.1 Materials

trans-4-hydroxy-2-nonenal (HNE), *trans*-4-hydroxy-2-hexenal (HHE), *trans*-4-hydroxy-2-dodecenal (HDE) and their respective acetal derivatives *trans*-4-hydroxy-2-hexenal dimethylacetal (HHEA), *trans*-4-hydroxy-2-nonenal dimethylacetal (HNEA) , *trans*-4-hydroxy-2-dodecenal dimethylacetal (HDEA) were synthesized as previously described [27]. *trans*-2-hexenal (HE), *trans*-2-nonenal (NE), *trans*-2-dodecenal (DE), hexanal (HA), nonanal (NA) and dodecanal (DA) were purchased from Sigma-Aldrich. Table 1 shows the main chemical characteristics of the molecules. All molecules were solubilized in DMSO before use and the final percentage of DMSO in culture medium was kept at 0.3% (v/v) to avoid any direct effect of DMSO on cell viability.

2.2 Cell culture

L6 C5 muscle cells (*Rattus norvegicus*) were obtained from the American Type Culture Collection (CRL 1458; Rockville, MD). Cells were grown in Dulbecco's modified Eagle's medium (DMEM, Sigma-Aldrich) containing 100 units/ml penicillin, 100 µg/ml streptomycin, 10% (v/v) fetal calf serum (FCS), and 2 mM glutamine. Cultures were maintained at 37°C in a humidified atmosphere containing 5% (v/v) CO_2. All cell treatments were realized in serum-free DMEM during 16 hours at concentrations ranging from 1 µM to 5 mM.

2.3 Cytotoxicity assay

Cell survival was quantified by colorimetric MTT assay, which measures mitochondrial activity in living cells. This method is based on the conversion of the 3-(4,5-dimethylthiazol-2-yl)-2,5-diphenyl-tetrazolium bromide to MTT-formazan crystal by mitochondrial enzymes. Cells seeded at a density of 3000 per well in a 96-well plate were allowed to adhere and stabilize overnight in DMEM containing 10% (v/v) FCS. Cells were then washed with PBS and treated with 4-hydroxy-2-alkenals or derivatives for 16 hours in serum-free DMEM. MTT assay (Cell Proliferation Kit I, Roche) was performed according to manufacturer instructions. The formazan dye produced by viable cells was quantified in a microplate reader at an absorbance of 560 nm, with a reference wavelength of 690 nm. Results were expressed as percent of the control.

2.4 Necrosis: Lactate dehydrogenase activity

Necrosis was estimated as function of the amount of lactate dehydrogenase (LDH) released in the medium compared to total extracellular plus intracellular content. L6 cells were seeded onto 96-well plates (3000 cells/well) and allowed to adhere overnight. Cells were then washed with PBS and treated with the tested molecules for 16 hours in serum-free DMEM. After treatment, the medium was collected and cells were lysed with 1% (v/v) Triton X100 for intracellular LDH measurement. The amount of LDH released by cells was determined using LDH-cytotoxicity test kit according to manufacturer's protocol (*In vitro* toxicology assay kit, LDH based, Sigma-Aldrich). The absorbance of samples was measured at 490 nm with a reference wavelength of 690 nm. Ratios of extracellular on total (extracellular + intracellular) LDH were expressed as percentage of the control value specified in each experiment.

2.5 Apoptosis: Caspase-3 activity

Apoptosis was estimated as function of the caspase-3 activity within the cells using commercially available kit (Caspase-3 Colorimetric Assay Kit, Biovision, Clinisciences, Montrouge, France). L6 cells were seeded onto 6-well plates and allowed to adhere overnight. Cells were then washed with PBS and treated with the tested molecules for 16 hours in serum-free DMEM. Cells were lysed and apoptosis was measured according to the manufacturer's protocol. Caspase-3 activity was normalized to the total amount of proteins within the cells and expressed as percent of untreated control.

2.6 Spectrophotometric DNPH assay for protein carbonyl content.

Protein carbonyl groups were detected using 2,4-dinitrophenylhydrazine (2,4-DNPH) as previously described [28]. Bovine serumalbumin (BSA, fraction V, Sigma Aldrich) 0.4% (w/v) was incubated for 2 hours at 37°C with 1 mM of each derivative. Carbonyl content was determined from the absorbance at 370 nm using a molar absorption coefficient of 22,000 $M.1cm^{-1}$ and normalized for the protein concentration measured by absorbance at 280 nm.

2.7 Physico-chemical parameters and 2D molecular descriptors.

All physico-chemical parameters and 2D molecular descriptors were calculated from the web-based PreADMET application (*http://preadmet.bmdrc.org*) and classified in four categories. **1) Constitutional descriptors:** All descriptors in this category are based on the number of atoms and chemical groups within the molecule. They describe the number of C=C and C=O double bonds, carbon and oxygen atoms, OH groups and molecular weight. **2) Physicochemical descriptors:** LogP defined as the octanol-water partition coefficient, is a measurement of molecular hydrophobicity. LUMO refers to the lowest unoccupied molecular orbital, according to the Frontier Orbital Theory and is used to quantify electrophilic reactivity. Polarizability characterizes how readily the atomic or molecular charge distribution is distorted by external static or oscillating electromagnetic fields. **3) Geometrical descriptors:** Hydrophobic surface area is defined as the total hydrophobic surface area divided by the total molecular solvent-accessible surface area, calculated for both unsaturated and saturated surfaces. Polar surface area and H-bond surface area are calculations of topological polar surface area based on fragment contributions. **4) Electrostatic descriptors:** Partial negative surface area (PNSA3) and partial positive surface area (PPSA3) are respectively defined as the sum of the solvent-accessible surface area of all negatively and positively charged atoms. The surface weighted charged partial surface area WNSA3, is defined as (PNSA3*TMSA/1000) where TMSA is the total molecular surface area. Difference in atomic charge weighted surface area (DPSA3) is defined as (PPSA3-PNSA3).

2.8 Statistical analysis and quantitative structure–toxicity relationships (QSTR)

Data are presented as means ± SEM. All data were analyzed and LC50 calculated using Prism v5.0 (GraphPad softwares, La Jolla, USA). LDH activity and carbonyl assay were compared using ANOVA. Differences were considered significant at the $P<0.05$ level. Quantitative structure activity relationships (QSTR) were derived by simple linear regression analysis using GraphPad Prism v5. The quality of the fit was characterized by the Pearson's correlation (r) and the probability of falsely rejecting the null hypothesis (P). The theoretically most significant equation should contain the

highest r^2 and the lowest P-value. Multilinear regression analysis for MTT, LDH activity and Caspase 3 activity data was performed using open source "R" software (www.r-project.org).

3 Results

3.1 4-hydroxy-2-alkenal induced Cytotoxicity

Estimation of deleterious effects on L6 cells viability was performed using the MTT test as described in methods. All molecules were tested in a large range of concentration for 16-hour treatment, and concentrations decreasing viability by 50% (Lethal Concentration, LC50) were calculated from a non-linear fit of each curve. Incubation of L6 muscle cells with all compounds resulted in a concentration-dependent decrease in cell viability. 4-hydroxy-2-alkenals were far more toxic than all other derivatives (Fig.1A). *trans*-4-hydroxy-2-dodecenal (HDE), having the longest carbon chain (C12) was the most toxic derivative, with an LC50 of 8.7 µM. *trans*-4-hydroxy-2-hexenal (HHE) showed an intermediate LC50 of 28.9 µM and *trans*-4-hydroxy-2-nonenal (HNE) was the derivative that affected the least cell viability with an LC50 of 53 µM. Acetal derivatives exhibited a lower toxicity than 4-hydroxy-2-alkenals (Fig.1B). Among them, *trans*-4-hydroxy-2-dodecenal dimethylacetal (HDEA) and *trans*-4-hydroxy-2-hexenal dimethylacetal (HHEA) were the most toxic with an LC50 of 120 µM and 128 µM respectively. The acetal derivative of HNE was by far the least toxic of these derivatives with an LC50 of 665 µM. *trans*-2-alkenals, exhibited a lower toxicity than 4-hydroxy-2-alkenals but stronger than acetals derivatives for C9 and C12 (Fig.1C). Thus *trans*-2-dodecenal (DE) was the most toxic with an LC50 of 50 µM. *trans*-2-hexenal (HE) exhibited an intermediate LC50 of 191 µM and *trans*-2-nonenal (NE) was the least toxic with an LC50 of 339 µM. As expected, alkanals exhibited the highest LC50 and therefore were the least toxic of all tested molecules (Fig.1D). For the latter derivatives, the most toxic was dodecanal (DA) with an LC50 of 552 µM followed by hexanal (HA) with an LC50 of 816 µM. The least toxic derivative was nonanal (NA) with an LC50 of 1175 µM. To summarize, the most toxic derivatives within each class of chemically-related compounds were always the C12 ones and the least toxic were the C9 ones. All calculated LC50 are summarized in table 2.

3.2 Mechanisms of 4-hydroxy-2-alkenal induced cytotoxicity

The decrease in cell viability measured by MTT may be due to many factors, as lipid peroxidation can lead to disruption of membranes and cell death. On one hand, the damage of mitochondria may lead to apoptosis while, on the other hand, rupture of plasma membrane may result in necrosis. We therefore estimated necrosis and apoptosis in L6 cells after treatment with all chemical derivatives.

Necrosis

Necrosis was estimated by the LDH release from cells. After treatment of cells with the LC50 calculated above, C6 derivatives exhibited no effects whereas all C12 derivatives, except HDE, affected LDH release (Fig. 2A). HDEA, DE and DA induced a 40%, 20% and 75% increase in LDH release, respectively. The LC50 of C9 derivatives, except for HNE, induced an equal and significant increase of 40% in LDH release. To sum up, neither the C6 derivatives nor hydroxy-alkenals increased membrane permeability when used at LC50. The other derivatives tested induced a significant increase in LDH release which could explain some of their toxic effects by induction of necrosis. To confirm these results, we treated L6 cells with the same concentration (100 µM) of each derivative and measured the release of LDH under these conditions (fig. 2B). LDH release was increased significantly for all hydroxy-alkenals, by 288, 202 and 213% for HHE, HNE and HDE, respectively. C12 derivatives also induced a significant increase in necrosis by 154, 154 and 176% for HDEA, DE and DA, respectively. Except for HHE and HNE, all other C6 and C9 derivatives did not affect necrosis.

Apoptosis

Apoptosis was estimated through the measurement of caspase-3 activity. Treatment of cells with the LC50 calculated above did not induced apoptosis (fig. 2C). We further measured the caspase-3 activity in L6 cells treated with 100 µM of each derivative (fig. 2D). Under this condition, caspase-3 activity was increased significantly by HHE and HDE, by 300 and 120% respectively. The C12 derivatives DE and DA also induced a significant increase by respectively 80 and 50% but no other derivatives did affect apoptosis.

After treatment with 100 µM of chemical derivatives, a highly significant correlation (r^2=0.696, $p<0.001$) was found between viability and necrosis (fig. 2E) but such a correlation could not be found between viability and apoptosis (fig. 2F). A multilinear regression was performed in order to show the correlations between viability, apoptosis and necrosis (see supplementary figure 1) and altogether, these results demonstrate that reduced viability is rather due to membrane disruption and necrosis than induction of apoptosis.

Protein carbonylation

As toxicity seems to depend on adducts formation, we used the carbonylation of bovine serum-albumin (BSA) as an index of the ability of molecules to form covalent adducts with proteins. BSA (0.4%, w/v) was incubated for 16 hours with 1 mM aldehydes, a concentration responsible for a dramatic decrease in L6 cells viability induced by all derivatives. Carbonyls were assayed using the DNPH assay described in methods. The highest amount of carbonyl groups in BSA was obtained after treatment with hydroxy-alkenals (Fig. 3A). HHE, HNE and HDE carbonyls on BSA were 100,

142 and 155 nmol/mg proteins respectively. Adduction by acetals derivatives was not significant with HHEA but was detectable with HNEA and HDEA: 38 and 105 nmol/mg proteins respectively. *trans*-2-alkenals exhibited an intermediate capacity of adduction: 57, 53 and 80 nmol/mg proteins for HE, NE and DE respectively. Conversely, no significant adduction of BSA was detected after treatment with alkanals. As expected, the quantity of adducts formed on BSA was correlated with the number of Michael acceptors (r^2=0.47, p=0.017). More interestingly, a strong negative correlation (r^2=0.769, p<0.001) was found between the logLC50 calculated from Fig. 1 and the carbonylation of BSA (Fig. 3B). This indicates that ability of molecules to form covalent adducts is a major determinant of their toxicity.

3.3 QSTR analysis for 4-hydroxy-2-alkenal induced cytotoxicity

Several molecular descriptors were calculated for each derivative from the preAdmet software and tested for correlation with the LC50 obtained from Figure 1. Constitutional descriptors chosen were the number of C=C and C=O double bonds, the number of OH groups and carbon atoms (carbon chain length), the molecular weight, and the number of Michael acceptors. The only descriptors that slightly correlate with LC50 were the number of C=C double bonds (r^2=0.43, p=0.02) and Michael acceptors (r^2=0.46, p=0.015), indicating that the toxicity of these derivatives could be related to their ability to form covalent adducts (especially Michael adducts). We failed to find any correlations of logLC50 with polarizability or octanol-water partition coefficient (LogP) which means that the toxicity of these different derivatives is not due to different sensitivity to electromagnetic deformation or solubility in medium. All compounds were soft electrophiles (LUMO<2.5 eV) but among the derivatives tested, 4-hydroxy-2-alkenals and *trans*-2-alkenals were the strongest electrophiles, which means that LUMO energy was smaller than those of other class members. On the basis of their respective quantum mechanical parameters, acetal derivatives and aldehydes were substantially weaker electrophiles. Nevertheless, we failed to find a correlation between LUMO energy and toxicity. Partial negative surface area (PNSA3, r^2=0.769, P=2.10^{-4}) and surface weighted charged partial negative surface area (WNSA3, r^2=0.425, P=0.022) were both highly correlated with logLC50 (Fig. 4 A-B).

Based on their chemical structure, acetal derivatives are not able to form covalent adducts on proteins. Nevertheless, we showed a significant adduction of BSA with these derivatives suggesting that the toxicity of these derivatives was due to spontaneous hydrolysis leading to the formation of parent 4-hydroxy-2-alkenals (see supplementary Figure 2). We thereafter considered acetal derivatives as outliers and re-calculated all correlations between logLC50 and chemical descriptors after exclusion of HHEA, HNEA and HDEA (Table 3). The number of C=C double bonds remains

correlated with log LC50 (r^2=0.604, P=0.014) and new correlations were found between logLC50 and the number of oxygen atoms or OH groups (r^2=0.640, P=0.010). LUMO was also correlated with the logLC50 (r^2=0.657, P=0.008) when using only 4-hydroxy-2-alkenals, *trans*-2-alkenals and alkanals. Geometrical descriptors correlated with logLC50 were the H-bond surface area (r^2=0.6406, P=0.0096) and the hydrophobic surface area for unsaturated groups (r^2=0.6041, P=0.0137) while the hydrophobic surface area for unsaturated groups was not significant. Partial negative surface area (PNSA3, r^2=0.855, $P=4\times10^{-4}$), partial positive surface area (PPSA3, r^2=0.852, $P=4\times10^{-4}$) and difference between PPSA and PNSA (DPSA3, r^2=0.880, $P=2.10^{-4}$) were both highly correlated with logLC50 (Fig.5). These three electrostatic descriptors show that the more electronegative groups there are in the molecule, the more cytotoxic it is. This can be explained by increased electron deficiency of the C=C double bond induced by both OH and C=O groups.

The 2D molecular descriptors shown in Supplementary Table 1 were used to derive a one-parameter model for QSTR to describe the cytotoxicity of hydroxy-alkenal derivatives. The electrostatic descriptor PNSA3 show the highest correlation with logLC50 (n=12, r^2=0.771 and $P=2\times10^{-4}$) and was therefore used as a one-term model for Quantitative Structure Toxicity Relationship to describe the toxicity of aldehydes towards L6 cells:

$$\mathbf{logLC50 = 4.522\ (\pm\ 0.412) + 0.210\ (\pm\ 0.036).PNSA3} \quad (1)$$

After exclusion of acetal derivatives from the analysis, cytotoxicity of hydroxy-2-alkenals derivatives was also correlated, with the physicochemical descriptors LUMO:

$$\mathbf{logLC50 = 2.083\ (\pm\ 0.153) - 1.079\ (\pm\ 0.293)\ .\ LUMO} \quad (2)$$

where n=9, r^2=0.660 and P=0.008. The partial negative surface area (PNSA3) and partial positive surface area (PPSA3), respectively defined as the sum of the solvent-accessible surface area of all negatively and positively charged atoms where also correlated with logLC50:

$$\mathbf{logLC50 = 4.489\ (\pm\ 0.378) - 0.212\ (\pm\ 0.033)\ .\ PNSA3} \quad (3)$$

$$\mathbf{logLC50 = 3.591\ (\pm\ 0.248) + 0.270\ (\pm\ 0.043)\ .\ PPSA3} \quad (4)$$

where n=9, r^2=0.85 and $P=4\times10^{-4}$ for both descriptors. Difference in atomic charge weighted surface area (DPSA3); defined as (PPSA3-PNSA3) exhibited the highest correlation with logLC50:

$$\mathbf{logLC50 = 4.156\ (\pm\ 0.294) + 0.123\ (\pm\ 0.017)\ .\ DPSA3} \quad (5)$$

where n=9, r^2= 0.880 and P= 2×10^{-4}.

4 Discussion

This study was focused on 4-hydroxy-2-alkenals and aimed to explain the mechanism of their toxicity by comparison to chemically related compounds. In the present study, we used several assays to test the ability of the different compounds to induce cytotoxicity. Viability was measured by MTT test, which depends on the capacity of mitochondria to metabolize MTT, and does not directly evaluate cell death. We therefore assessed both apoptosis and necrosis induced by the derivatives and demonstrated that toxicity of derivatives can be better explained by necrosis than apoptosis. We used acetal derivatization to mask the aldehyde group and prevent Schiff base formation as well as Michael addition. Thus, a low toxicity was expected for these compounds. Interestingly, dimethylacetal derivatives still exhibited a 10-fold higher LC50 compared to parent hydroxy-alkenals. This remaining toxicity could be explained by hydrolysis of acetal derivatives, therefore leading to parent 4-hydroxy-2-alkenals release (see Supplementary Figure 2). The deletion of the double bond conjugated with the aldehyde group in alkanals dramatically blunted the toxicity, indicating that Michael adducts formation is a crucial determinant of hydroxy-alkenals toxicity. The absence of alpha-hydroxyl group led to a decreased toxicity which matched acetal derivatives. In hydroxyalkenals, the presence of the hydroxyl group close to the double bond appears to strengthen the toxicity. This enhancing effect could be linked to increased solubility of these aldehydes. LC50 was not correlated with LogP, we may however hypothesize that these molecules may have different targets, being either plasma membranes or intracellular compartments. This would be coherent with the results obtained on LDH activity which shows that chemical derivatives do not alter viability in the same way. Different sites of adduction could have different effects on viability and thus could explain part of the differences observed. More likely, the presence of OH groups could enhance double bond electropositivity and therefore increased reactivity and nucleophilic attack potencies. In favor of the latter possibility, PNSA3, PPSA3 and DPSA3 were highly correlated with logLC50 and we demonstrated that they could be good predictors for aldehyde toxicity (see Supplementary Table 2).

Interestingly, within each group of chemically related compounds, the most toxic was always the C12 and the less toxic was always the C9 derivatives. Consequently, no correlation could be found

with molecular weight or number of carbons but this difference clearly demonstrated that carbons chain length is an important parameter in lipid aldehyde cytoxicity. It could affect hydrophobic / hydrophilic balance leading to possible different effects or targets or could affect detoxification by enzymes and/or antioxidants systems. In favor of the second possibility, several enzymes such as glutathione S-transferase or aldehyde dehydrogenase are in charge of the detoxification of aldehydes, but acrolein, hexenal or decadienal are not metabolized with the same affinity by these enzymes [29-32]. Moreover, it has recently been shown that 4-HHE was metabolized by reduced glutathione at a higher rate than 4-HNE in cerebral cortex and hippocampus [33].

Hydroxy-alkenals are alpha-beta-unsaturated carbonyl derivatives, and as such, are composed of a carbon-carbon double bond linked to an electron-withdrawing carbonyl group. The resulting combination of polarizable mobile electrons and electron-withdrawing capacity creates an area of electron deficiency at the beta-carbon atom. Therefore, hydroxy-alkenals are electrophiles (electron-deficient species), which is the case of many *in vivo* toxicants that covalently interact with biological nucleophilic targets such as amino-acids [34-36]. In the present study, all compounds tested were soft electrophiles, as defined by the level of LUMO energy lower than 2.5 eV. The respective quantum mechanical values indicate the following rank order of derivatives electrophilicity: hydroxy-alkenals > *trans*-2-alkenals >> aldehydes > acetals. Generally, the spectrum of electrophilicity is closely correlated to *in vitro* toxic potencies [37] and we found such a correlation under our conditions after exclusion of acetal outliers. Moreover, we found a positive correlation between the logLC50 and the number of C=C bonds and Michael acceptors. This pointed out the fact that toxicity may be related to Michael adducts formation, which was confirmed by analysis of covalent adducts formation on BSA by chemical derivatives. Adduction ability was ranked: HDE > HNE > HHE ≈ HDEA > DE > HE ≈ NE > HNEA > HHEA ≈ HA ≈ NA ≈ DA. This ability to form covalent adducts with BSA was highly correlated with the calculated logLC50 (Fig. 3). Altogether, these results confirm that toxicity of hydroxy-alkenals and chemically related aldehydes is mainly due to adduct formation within the cells. Our study was focused on protein adducts, however, formation of adducts on nucleic acids or phospholipids by hydroxy-alkenals have also been described. These adducts results from both Michael addition or Schiff base formation through the same mechanism we described above, and may contribute to the deleterious effects of aldehydes we observed [20,22,38,39].

There is considerable evidence that oxidative stress and subsequent lipid peroxidation are major aspects of several diseases including alcoholic liver damage, atherosclerosis, and Alzheimer's

disease [1,2,40,41] and that these processes are mediated at least in part by the release of toxic lipid aldehydes [42,43]. Moreover, many aldehydes derivatives are heavily present in tissues in pathophysiologic conditions and exhibit various biological effects. This is the case for HHE and HNE, but also for *trans*-2-hexenal, *trans*-2-nonenal, hexanal and nonanal [8,44-46]. Several other endogenous aldehydes like crotonaldehyde, acrolein or malondialdehyde (MDA) share part of their structure with hydroxy-alkenals and may also be deleterious through adduct formation on proteins, DNA or phospholipids [47-49]. As a matter of fact, such aldehydes could reach micromolar concentration under oxidative stress conditions [50,51], which is relevant to cell damage in response to adduct formation.

5 Conclusion

Lipid peroxidation is one of the most important sources of endogenous toxic by-products. Our study points out the fact that 4-hydroxy-2-alkenals dramatic effects on cell viability are due to their peculiar structure making them able to form covalent adducts, particularly Michael adducts, on biomolecules. In fact, toxicity of 4-hydroxy-2-alkenals was strongly correlated with parameters related to their electrophilicity. We also point out the deleterious effects of lipid aldehydes on cell viability at low concentration through induction of both apoptosis and necrosis, and therefore show the important implication of lipid peroxidation by-products in oxidative stress injury. Finally, our study suggests that protection against these electrophiles compounds could be achieved by using nucleophilic scavengers such as *N*-acetylcysteine or hydralazine [52] and might be of possible therapeutic value in oxidative stress associated pathologies.

ACKNOWLEDGMENT

This work was supported by INSERM and INSA-Lyon. N. PILLON was supported by grants from the French « Ministère de l'Education Nationale, de la Recherche et de la Technologie » and B. Caré was supported by grants from « Région Rhône-Alpes ». The authors gratefully acknowledge Dr Pedro Da Silva for fruitfull discussion about 2D and 3D QSAR models.

CONFLICT OF INTEREST STATEMENT

The authors declare no conflict of interest.

BIBLIOGRAPHY

[1] R.A. Floyd, K. Hensley, Oxidative stress in brain aging. Implications for therapeutics of neurodegenerative diseases, Neurobiol Aging. 23 (2002) 795-807.
[2] R.A. Floyd, Antioxidants, oxidative stress, and degenerative neurological disorders, Proc Soc Exp Biol Med. 222 (1999) 236-45.
[3] A. Ceriello, E. Motz, Is oxidative stress the pathogenic mechanism underlying insulin resistance, diabetes, and cardiovascular disease? The common soil hypothesis revisited, Arterioscler. Thromb. Vasc. Biol. 24 (2004) 816-823.
[4] S. Furukawa, T. Fujita, M. Shimabukuro, M. Iwaki, Y. Yamada, Y. Nakajima, et al., Increased oxidative stress in obesity and its impact on metabolic syndrome, J Clin Invest. 114 (2004) 1752-61.
[5] V.N. Bochkov, O.V. Oskolkova, K.G. Birukov, A. Levonen, C.J. Binder, J. Stöckl, Generation and biological activities of oxidized phospholipids, Antioxid. Redox Signal. 12 (2010) 1009-1059.
[6] T. Grune, W.G. Siems, K. Schönheit, I.E. Blasig, Release of 4-hydroxynonenal, an aldehydic mediator of inflammation, during postischaemic reperfusion of the myocardium, Int J Tissue React. 15 (1993) 145-150.
[7] N. Bashan, J. Kovsan, I. Kachko, H. Ovadia, A. Rudich, Positive and negative regulation of insulin signaling by reactive oxygen and nitrogen species, Physiol Rev. 89 (2009) 27-71.
[8] A. Catalá, Lipid peroxidation of membrane phospholipids generates hydroxy-alkenals and oxidized phospholipids active in physiological and/or pathological conditions, Chem Phys Lipids. 157 (2009) 1-11.
[9] M. Guichardant, S. Bacot, P. Molière, M. Lagarde, Hydroxy-alkenals from the peroxidation of n-3 and n-6 fatty acids and urinary metabolites, Prostaglandins Leukot Essent Fatty Acids. 75 (2006) 179-82.
[10] W.A. Pryor, N.A. Porter, Suggested mechanisms for the production of 4-hydroxy-2-nonenal from the autoxidation of polyunsaturated fatty acids, Free Radic Biol Med. 8 (1990) 541-3.
[11] F.J. van Kuijk, L.L. Holte, E.A. Dratz, 4-Hydroxyhexenal: a lipid peroxidation product derived from oxidized docosahexaenoic acid, Biochim. Biophys. Acta. 1043 (1990) 116-118.
[12] E.K. Long, T.C. Murphy, L.J. Leiphon, J. Watt, J.D. Morrow, G.L. Milne, et al., Trans-4-hydroxy-2-hexenal is a neurotoxic product of docosahexaenoic (22:6; n-3) acid oxidation, J. Neurochem. 105 (2008) 714-724.
[13] Y. Ito, M. Arakawa, K. Ishige, H. Fukuda, Comparative study of survival signal withdrawal- and 4-hydroxynonenal-induced cell death in cerebellar granule cells, Neurosci Res. 35 (1999) 321-7.
[14] S. Choudhary, W. Zhang, F. Zhou, G.A. Campbell, L.L. Chan, E.B. Thompson, et al., Cellular lipid peroxidation end-products induce apoptosis in human lens epithelial cells, Free Radic Biol Med. 32 (2002) 360-9.
[15] A. Ishimura, K. Ishige, T. Taira, S. Shimba, S. Ono, H. Ariga, et al., Comparative study of hydrogen peroxide- and 4-hydroxy-2-nonenal-induced cell death in HT22 cells, Neurochem Int. 52 (2007) 776-85.
[16] A. Malecki, R. Garrido, M.P. Mattson, B. Hennig, M. Toborek, 4-Hydroxynonenal induces oxidative stress and death of cultured spinal cord neurons, J Neurochem. 74 (2000) 2278-87.
[17] W. Liu, M. Kato, A.A. Akhand, A. Hayakawa, H. Suzuki, T. Miyata, et al., 4-hydroxynonenal induces a cellular redox status-related activation of the caspase cascade for apoptotic cell death, J Cell Sci. 113 (Pt 4) (2000) 635-41.
[18] K. Uchida, M. Shiraishi, Y. Naito, Y. Torii, Y. Nakamura, T. Osawa, Activation of stress signaling pathways by the end product of lipid peroxidation. 4-hydroxy-2-nonenal is a potential inducer of intracellular peroxide production, J Biol Chem. 274 (1999) 2234-42.
[19] J. Ruef, M. Moser, C. Bode, W. Kubler, M.S. Runge, 4-hydroxynonenal induces apoptosis, NF-kappaB-activation and formation of 8-isoprostane in vascular smooth muscle cells, Basic Res

Cardiol. 96 (2001) 143-50.
[20] S. Bacot, N. Bernoud-Hubac, B. Chantegrel, C. Deshayes, A. Doutheau, G. Ponsin, et al., Evidence for in situ ethanolamine phospholipid adducts with hydroxy-alkenals, J Lipid Res. 48 (2007) 816-25.
[21] L.M. Sayre, D. Lin, Q. Yuan, X. Zhu, X. Tang, Protein adducts generated from products of lipid oxidation: focus on HNE and one, Drug Metab Rev. 38 (2006) 651-75.
[22] W. Hu, Z. Feng, J. Eveleigh, G. Iyer, J. Pan, S. Amin, et al., The major lipid peroxidation product, trans-4-hydroxy-2-nonenal, preferentially forms DNA adducts at codon 249 of human p53 gene, a unique mutational hotspot in hepatocellular carcinoma, Carcinogenesis. 23 (2002) 1781-9.
[23] R.J. Schaur, Basic aspects of the biochemical reactivity of 4-hydroxynonenal, Mol Aspects Med. 24 (2003) 149-59.
[24] P.A. Grimsrud, M.J. Picklo, T.J. Griffin, D.A. Bernlohr, Carbonylation of adipose proteins in obesity and insulin resistance: identification of adipocyte fatty acid-binding protein as a cellular target of 4-hydroxynonenal, Mol Cell Proteomics. 6 (2007) 624-37.
[25] T. Ishii, E. Tatsuda, S. Kumazawa, T. Nakayama, K. Uchida, Molecular basis of enzyme inactivation by an endogenous electrophile 4-hydroxy-2-nonenal: identification of modification sites in glyceraldehyde-3-phosphate dehydrogenase, Biochemistry. 42 (2003) 3474-3480.
[26] M.S. Cooke, M.D. Evans, M. Dizdaroglu, J. Lunec, Oxidative DNA damage: mechanisms, mutation, and disease, Faseb J. 17 (2003) 1195-1214.
[27] L. Soulère, Y. Queneau, A. Doutheau, An expeditious synthesis of 4-hydroxy-2E-nonenal (4-HNE), its dimethyl acetal and of related compounds, Chem Phys Lipids. 150 (2007) 239-43.
[28] R.L. Levine, N. Wehr, J.A. Williams, E.R. Stadtman, E. Shacter, Determination of carbonyl groups in oxidized proteins, Methods Mol. Biol. 99 (2000) 15-24.
[29] G. Eisenbrand, J. Schuhmacher, P. Gölzer, The influence of glutathione and detoxifying enzymes on DNA damage induced by 2-alkenals in primary rat hepatocytes and human lymphoblastoid cells, Chem. Res. Toxicol. 8 (1995) 40-46.
[30] H. Niknahad, A.G. Siraki, A. Shuhendler, S. Khan, S. Teng, G. Galati, et al., Modulating carbonyl cytotoxicity in intact rat hepatocytes by inhibiting carbonyl-metabolizing enzymes. I. Aliphatic alkenals, Chem. Biol. Interact. 143-144 (2003) 107-117.
[31] M. Fujita, M.Z. Hossain, Modulation of pumpkin glutathione S-transferases by aldehydes and related compounds, Plant Cell Physiol. 44 (2003) 481-490.
[32] M.W. Lamé, H.J. Segall, Metabolism of the pyrrolizidine alkaloid metabolite trans-4-hydroxy-2-hexenal by mouse liver aldehyde dehydrogenases, Toxicol. Appl. Pharmacol. 82 (1986) 94-103.
[33] E.K. Long, T.A. Rosenberger, M.J. Picklo, Ethanol withdrawal increases glutathione adducts of 4-hydroxy-2-hexenal but not 4-hydroxyl-2-nonenal in the rat cerebral cortex, Free Radic. Biol. Med. 48 (2010) 384-390.
[34] J.A. Hinson, D.W. Roberts, Role of covalent and noncovalent interactions in cell toxicity: effects on proteins, Annu. Rev. Pharmacol. Toxicol. 32 (1992) 471-510.
[35] T.W. Schultz, R.E. Carlson, M.T.D. Cronin, J.L.M. Hermens, R. Johnson, P.J. O'Brien, et al., A conceptual framework for predicting the toxicity of reactive chemicals: modeling soft electrophilicity, SAR QSAR Environ Res. 17 (2006) 413-428.
[36] R.M. LoPachin, T. Gavin, D.R. Petersen, D.S. Barber, Molecular mechanisms of 4-hydroxy-2-nonenal and acrolein toxicity: nucleophilic targets and adduct formation, Chem. Res. Toxicol. 22 (2009) 1499-1508.
[37] R.M. Lopachin, D.S. Barber, B.C. Geohagen, T. Gavin, D. He, S. Das, Structure-toxicity analysis of type-2 alkenes: in vitro neurotoxicity, Toxicol. Sci. 95 (2007) 136-146.
[38] U.C.S. Yadav, K.V. Ramana, Y.C. Awasthi, S.K. Srivastava, Glutathione level regulates HNE-induced genotoxicity in human erythroleukemia cells, Toxicol Appl Pharmacol. 227 (2008)

257-64.
[39] L.J. Marnett, Oxyradicals and DNA damage, Carcinogenesis. 21 (2000) 361-370.
[40] N. Dierckx, G. Horvath, C. van Gils, J. Vertommen, J. van de Vliet, I. De Leeuw, et al., Oxidative stress status in patients with diabetes mellitus: relationship to diet, Eur J Clin Nutr. 57 (2003) 999-1008.
[41] A.I. Cederbaum, Y. Lu, D. Wu, Role of oxidative stress in alcohol-induced liver injury, Arch. Toxicol. 83 (2009) 519-548.
[42] M.U. Dianzani, 4-hydroxynonenal from pathology to physiology, Mol Aspects Med. 24 (2003) 263-72.
[43] A. Negre-Salvayre, C. Coatrieux, C. Ingueneau, R. Salvayre, Advanced lipid peroxidation end products in oxidative damage to proteins. Potential role in diseases and therapeutic prospects for the inhibitors, Br J Pharmacol. 153 (2008) 6-20.
[44] H. Esterbauer, G. Jurgens, O. Quehenberger, E. Koller, Autoxidation of human low density lipoprotein: loss of polyunsaturated fatty acids and vitamin E and generation of aldehydes, J. Lipid Res. 28 (1987) 495-509.
[45] I. Miwa, N. Ichimura, M. Sugiura, Y. Hamada, S. Taniguchi, Inhibition of glucose-induced insulin secretion by 4-hydroxy-2-nonenal and other lipid peroxidation products, Endocrinology. 141 (2000) 2767-72.
[46] B.G. Hill, P. Haberzettl, Y. Ahmed, S. Srivastava, A. Bhatnagar, Unsaturated lipid peroxidation-derived aldehydes activate autophagy in vascular smooth-muscle cells, Biochem J. 410 (2008) 525-34.
[47] X. Liu, Z. Yang, X. Pan, M. Zhu, J. Xie, Crotonaldehyde induces oxidative stress and caspase-dependent apoptosis in human bronchial epithelial cells, Toxicol. Lett. 195 (2010) 90-98.
[48] I.G. Minko, I.D. Kozekov, T.M. Harris, C.J. Rizzo, R.S. Lloyd, M.P. Stone, Chemistry and biology of DNA containing 1,N(2)-deoxyguanosine adducts of the alpha,beta-unsaturated aldehydes acrolein, crotonaldehyde, and 4-hydroxynonenal, Chem. Res. Toxicol. 22 (2009) 759-778.
[49] S.S. Hecht, E.J. McIntee, M. Wang, New DNA adducts of crotonaldehyde and acetaldehyde, Toxicology. 166 (2001) 31-36.
[50] L.T. McGrath, B.M. McGleenon, S. Brennan, D. McColl, S. McILroy, A.P. Passmore, Increased oxidative stress in Alzheimer's disease as assessed with 4-hydroxynonenal but not malondialdehyde, Qjm. 94 (2001) 485-90.
[51] K. Syslova, P. Kacer, M. Kuzma, V. Najmanova, Z. Fenclova, S. Vlckova, et al., Rapid and easy method for monitoring oxidative stress markers in body fluids of patients with asbestos or silica-induced lung diseases, J. Chromatogr. B Analyt. Technol. Biomed. Life Sci. (2009).
[52] R. Mehta, L. Wong, P.J. O'Brien, Cytoprotective mechanisms of carbonyl scavenging drugs in isolated rat hepatocytes, Chem. Biol. Interact. 178 (2009) 317-323.

Figure legends

Figure 1. Overnight treatments with 4-hydroxy-2-alkenals or derivatives decrease L6 muscle cell viability. Cells were treated for 16 hours with increasing concentrations (1 µM-5 mM) of 4-hydroxy-2-alkenals (A), acetal derivatives (B), *trans*-2-alkenals (C) or alkanals (D). Viability was measured by the MTT test as described in methods and expressed as non-linear fits of at least 6 different experiments. Data are mean ± SEM expressed as percent of untreated control. HHE: *trans*-4-hydroxy-2-hexenal, HNE: *trans*-4-hydroxy-2-nonenal, HDE: *trans*-4-hydroxy-2-dodecenal, HHEA: *trans*-4-hydroxy-2-hexenal dimethylacetal, HNEA: *trans*-4-hydroxy-2-nonenal dimethylacetal, HDEA: *trans*-4-hydroxy-2-dodecenal dimethylacetal, HE: *trans*-2-hexenal, NE: *trans*-2-nonenal, DE: *trans*-2-dodecenal, HA: hexanal, NA: nonanal, DA: dodecanal.

Figure 2. 4-hydroxy-2-alkenal induced necrosis and apoptosis in L6 muscle cells. Necrosis was estimated by the LDH release in the medium (ratio extracellular LDH /total LDH) and apoptosis by caspase-3 activity. **A)** Necrosis after a 16 hours treatment with the LC50 calculated from Figure 1. **B)** Necrosis after a 16 hours treatment with 100 µM of each derivative. **C)** Apoptosis after a 16 hours treatment with the LC50 calculated from Figure 1. **D)** Apoptosis after a 16 hours treatment with 100 µM of each derivative. **E)** Correlation between viability and necrosis in L6 muscle cells. **F)** Correlation between viability and apoptosis in L6 muscle cells. Results are mean ± Sd, expressed in percent of untreated control, $n \geq 3$, ***$p < 0.005$, significant difference from control, ns: non significant.

F**igure 3. 4-hydroxy-2-alkenals or derivatives produced covalent adducts on proteins.** Bovine serumalbumine 0.4% (w/v) was incubated for 16 hours with 1 mM of each derivative. Bovine serumalbumine adduct was estimated through the measurement of carbonyl content using dinitrophenylhydrazine as described in methods. Results are means ± SEM from 4 independent experiments, *$p < 0.05$, significant difference from control.

F**igure 4. Correlation between cytotoxicity of 4-hydroxy-2-alkenal derivatives and electrostatic descriptors partial negative surface area 3rd type (PNSA3) and surface weighted charged partial surface area 3rd type (WNSA3)**. A) PNSA3 is defined as the sum of the solvent-accessible surface area of all negatively charged atoms. B) WNSA3 is defined as (PNSA3*TMSA/1000) where

TMSA is the total molecular surface area. Both molecular electrostastic descriptors were calculated from the web-based PreADMET application as described in the methods section.

F**igure 5. 4-hydroxy-2-alkenal derivatives exhibited a strong correlation with some 2D electrostatic molecular descriptors when acetal derivatives are excluded from analysis.** Strong correlations were found between cytotoxicity and partial positive surface area 3rd type (PPSA3, **Fig 5A**), partial negative surface area 3rd type (PNSA3, **Fig 5B**) and difference in atomic charge weighted surface area (DPSA3, **Fig 5C**). 2D molecular electrostatic descriptors were calculated from the web-based PreADMET application as described in the methods section.

Table 1

Main chemical structures and characteristics of chemical derivatives

Name		MW (g/mol)	Linear Formula	Structure	LogP
trans -4-hydroxy-2-hexenal	HHE	114.1	$C_6H_{10}O_2$	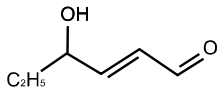	0.91
trans -4-hydroxy-2-nonenal	HNE	156.2	$C_9H_{16}O_2$	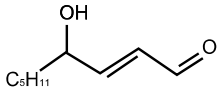	2.31
trans -4-hydroxy-2-dodecenal	HDE	198.3	$C_{12}H_{22}O_2$	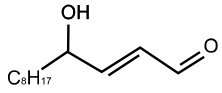	3.7
trans -4-hydroxy-2-hexenal dimethylacetal	HHEA	160.2	$C_8H_{16}O_3$	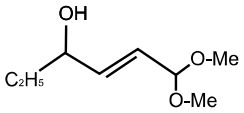	0.85
trans -4-hydroxy-2-nonenal dimethylacetal	HNEA	202.3	$C_{11}H_{22}O_3$	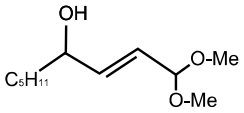	2.24
trans -4-hydroxy-2-dodecenal dimethylacetal	HDEA	244.4	$C_{14}H_{28}O_3$	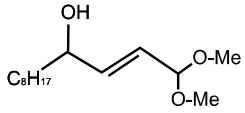	3.63
trans-2-hexenal	HE	98.1	$C_6H_{10}O_1$	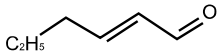	1.93
trans-2-nonenal	NE	140.2	$C_9H_{16}O_1$	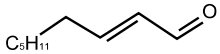	3.32
trans-2-dodecenal	DE	182.3	$C_{12}H_{22}O_1$	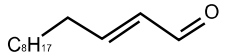	4.71
hexanal	HA	100.2	$C_6H_{12}O_1$	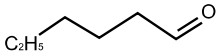	2.28
nonanal	NA	142.2	$C_9H_{18}O_1$	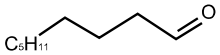	3.68
dodecanal	DA	184.3	$C_{12}H_{24}O_1$	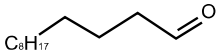	5.07

LogP (octanol-water partition coefficient) was calculated from the online preAdmet software. MW= Molecular Weight.

Table 2

LC50 calculated from the MTT assay

Name	LC50 (µM)	logLC50	95% Confidence Intervals
trans -4-hydroxy-2-hexenal	28.9 ± 1.1	1.461	1.399 to 1.523
trans -4-hydroxy-2-nonenal	53.0 ± 1.1	1.725	1.667 to 1.783
trans -4-hydroxy-2-dodecenal	8.7 ± 1.1	0.938	0.860 to 1.016
trans -4-hydroxy-2-hexenal dimethylacetal	128.6 ± 1.2	2.109	1.937 to 2.282
trans -4-hydroxy-2-nonenal dimethylacetal	665.1 ± 1.1	2.823	2.744 to 2.902
trans -4-hydroxy-2-dodecenal dimethylacetal	120.6 ± 1.3	2.081	1.837 to 2.326
trans-2-hexenal	191.1 ± 1.2	2.281	2.126 to 2.437
trans-2-nonenal	339.7 ± 1.2	2.531	2.356 to 2.706
trans-2-dodecenal	50.7 ± 1.4	1.705	1.435 to 1.974
hexanal	816.1 ± 1.1	2.912	2.841 to 2.982
nonanal	1175.0 ± 1.1	3.070	3.015 to 3.125
dodecanal	552.5 ± 1.1	2.742	2.696 to 2.789

L6 muscle cells were treated for 16 hours with increasing doses of chemical derivatives in serum-free conditions. Viability was measured with the MTT assay and LC50 were calculated using non linear fit. Results are means from at least 5 independent experiments.

Table 3

QSTR analysis of hydroxy-alkenal toxicicty: Correlations of logLC50 with 2D molecular descriptors for 4-hydroxy-2-alkenals, *trans*-2-alkenals and akanals, after exclusion of acetal derivatives.

Constitutional descriptors	**Pearson r**	**95% confidence interval**	**P value (two-tailed)**	**P value summary**	**R squared**
Molecular weight	-0.395	-0.8392 to 0.3648	0.2924	ns	0.1562
No. C=C bonds	-0.777	-0.9507 to -0.2337	0.0137	*	0.6041
No. alcohol groups	-0.800	-0.9562 to -0.2901	0.0096	**	0.6402
No. C atoms	-0.249	-0.7838 to 0.4972	0.5174	ns	0.0622
No. O atoms	-0.801	-0.9562 to -0.2901	0.0096	**	0.6402

Physicochemical descriptors	**Pearson r**	**95% confidence interval**	**P value (two-tailed)**	**P value summary**	**R squared**
SK MP (SK atomic types. centigrade)	-0.896	-0.9782 to -0.5742	0.0011	**	0.8037
LUMO energy	0.811	0.3168 to 0.9586	0.0081	**	0.6569
Water solvation free energy	0.789	0.2640 to 0.9537	0.0113	*	0.6237
logP	-0.337	-0.8179 to 0.4220	0.3758	ns	0.1133
Polarizability	-0.299	-0.8035 to 0.4560	0.4350	ns	0.0892

Geometrical descriptors	**Pearson r**	**95% confidence interval**	**P value (two-tailed)**	**P value summary**	**R squared**
H-bond surface area (Polar surface area)	-0.800	-0.9562 to -0.2901	0.0096	**	0.6402
Hydrophobic surface area (unsaturated group)	-0.777	-0.9507 to -0.2337	0.0137	*	0.6041
Hydrophobic surface area (saturated group)	0.045	-0.6382 to 0.6887	0.9083	ns	0.0020

Electrostatic descriptors	**Pearson r**	**95% confidence interval**	**P value (two-tailed)**	**P value summary**	**R squared**
PNSA3 (partial negative surface area 3rd type)	0.924	0.6740 to 0.9843	0.0004	***	0.8545
PPSA3 (partial positive surface area 3rd type)	-0.923	-0.9840 to -0.6684	0.0004	***	0.8518
DPSA3 (PPSA3 - PNSA3)	-0.938	-0.9872 to -0.7269	0.0002	***	0.8801

Molecular descriptors were calculated from the preAdmet software and tested for correlation with the logLC50 calculated from the MTT assay. Statistical significance at $p<0.05$ was determined using the Prism software.

Figure 1

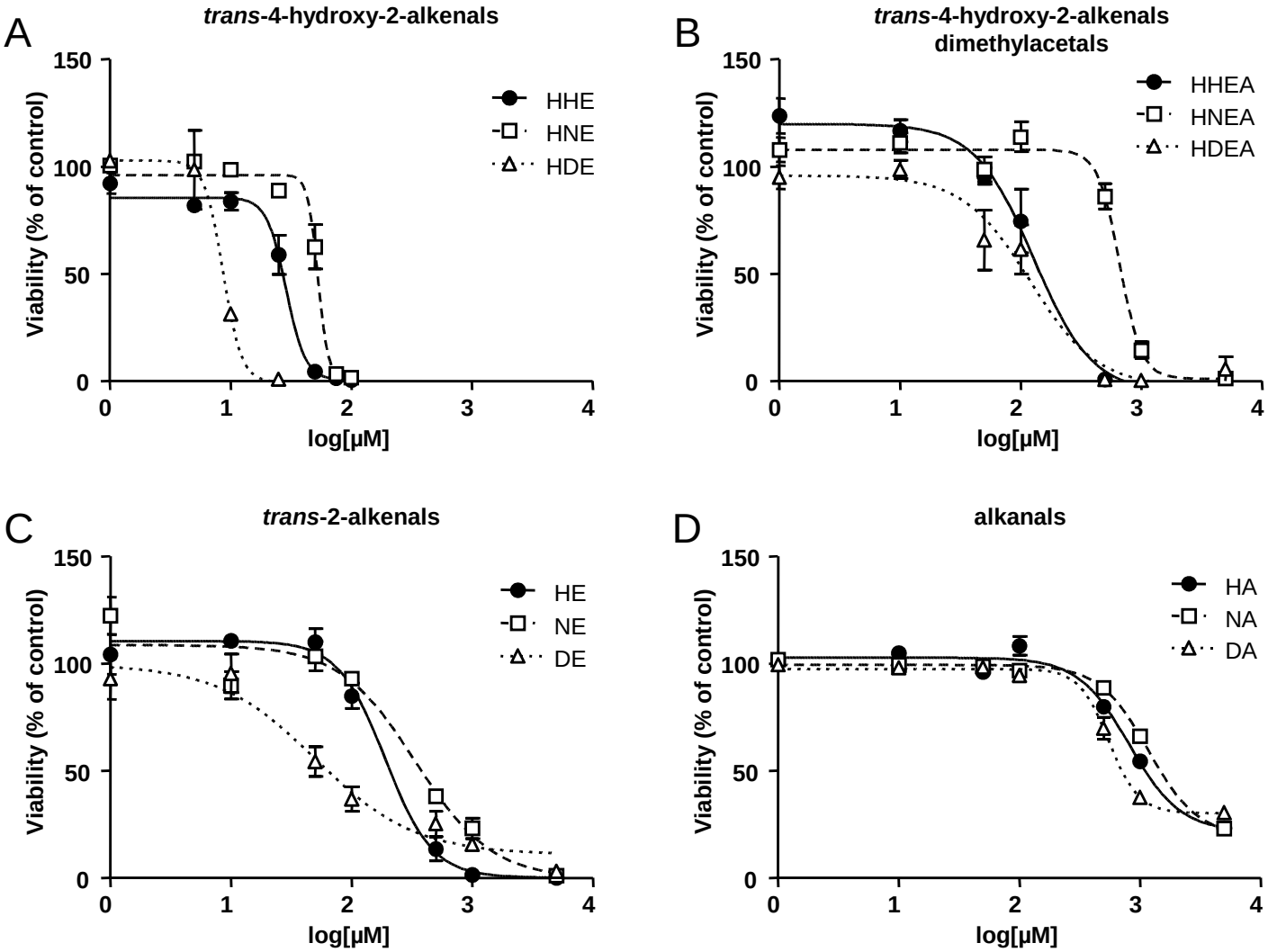
A
trans-4-hydroxy-2-alkenals
Viability (% of control)
log[μM]
HHE
HNE
HDE
B
trans-4-hydroxy-2-alkenals
dimethylacetals
HHEA
HNEA
HDEA
C
trans-2-alkenals
HE
NE
DE
D
alkanals
HA
NA
DA

Figure 2

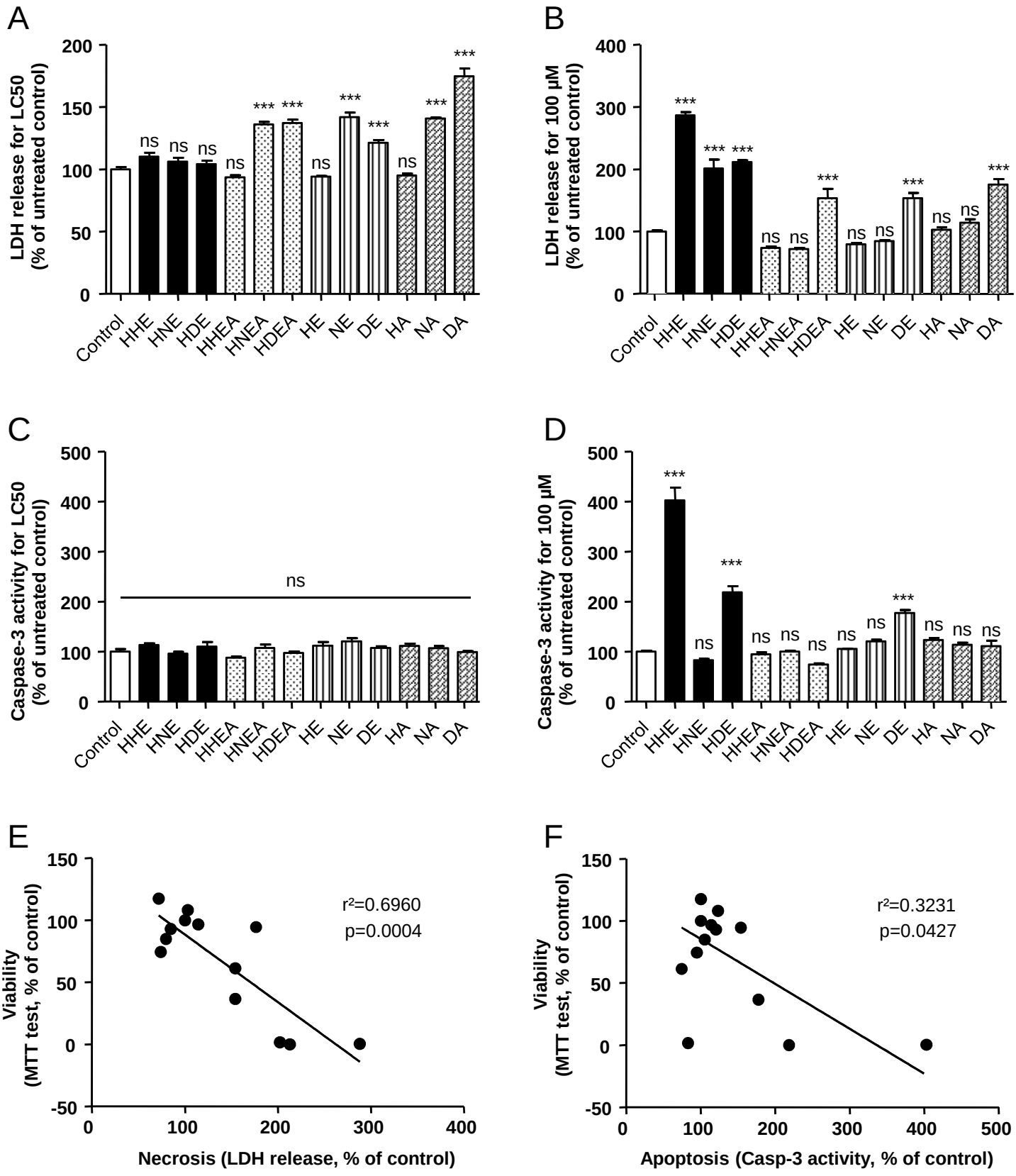
A
LDH release for LC50 (% of untreated control)
B
LDH release for 100 µM (% of untreated control)
C
Caspase-3 activity for LC50 (% of untreated control)
D
Caspase-3 activity for 100 µM (% of untreated control)
Control
HHE
HNE
HDE
HHEA
HNEA
HDEA
HE
NE
DE
HA
NA
DA
ns
***
E
Viability (MTT test, % of control)
Necrosis (LDH release, % of control)
r²=0.6960
p=0.0004
F
Viability (MTT test, % of control)
Apoptosis (Casp-3 activity, % of control)
r²=0.3231
p=0.0427

Figure 3

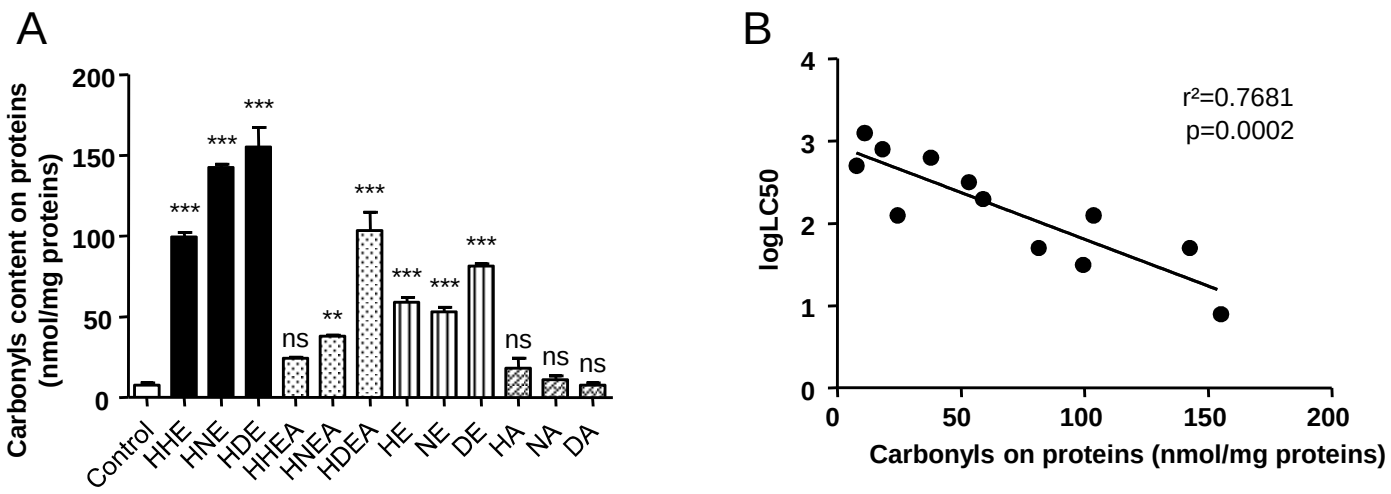
A
Carbonyls content on proteins (nmol/mg proteins)
200
150
100
50
0
***
***
***
ns
**
***
***
***
***
ns
ns
ns
Control
HHE
HNE
HDE
HHEA
HNEA
HDEA
HE
NE
DE
HA
NA
DA
B
logLC50
4
3
2
1
0
r²=0.7681
p=0.0002
0
50
100
150
200
Carbonyls on proteins (nmol/mg proteins)

Figure 4

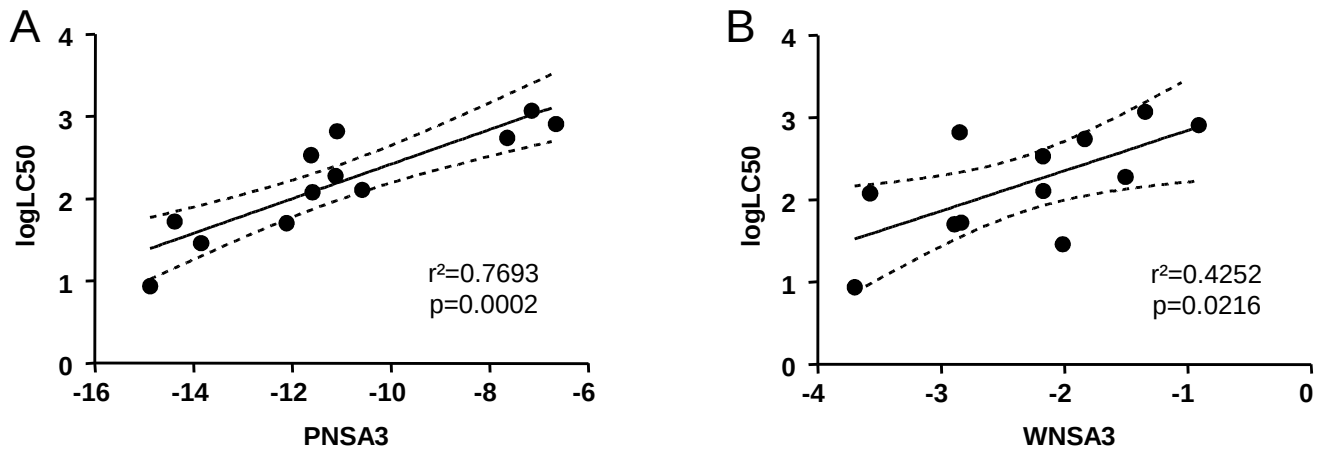
A
B
logLC50
PNSA3
WNSA3
r²=0.7693
p=0.0002
r²=0.4252
p=0.0216
4
3
2
1
0
-16
-14
-12
-10
-8
-6
-4
-3
-2
-1
0

Figure 5

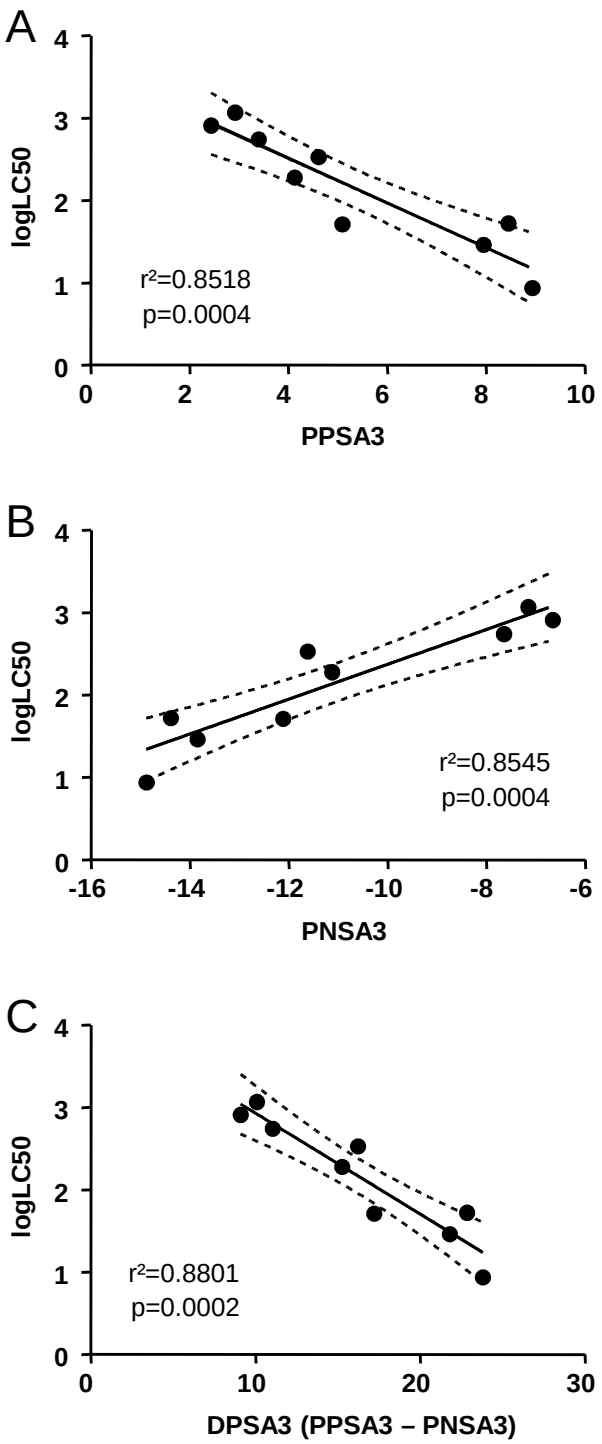
A
logLC50
PPSA3
r²=0.8518
p=0.0004
B
logLC50
PNSA3
r²=0.8545
p=0.0004
C
logLC50
DPSA3 (PPSA3 – PNSA3)
r²=0.8801
p=0.0002

Supplementary Figure legends

S**upplementary Figure 1: Multilinear regression model of aldehydes-induced cell death.** Viability was measured by MTT test, Necrosis by LDH release and Apoptosis by caspase-3 activity after a 16 hours treatment with 100 µM of chemical derivatives. Note that hydroxy-alkenal induced cytotoxicty result from necrosis rather from apoptosis.

S**upplementary Figure 2: spontaneous hydrolysis of *trans*-4-hydroxy-2-alkenals dimethylacetals in ultrapure water.** *trans*-4-hydroxy-2-alkenals exhibit a typical UV spectrum with a maximum absorption for 234 nm while acetal derivatives exhibit no absorption for this wavelength. Based on this difference, hydrolysis of HNEA was followed by increase in the 234 nm absorbance due to HNE apparition. Measurement of HNEA spectrum was performed after 0, 10, 30, 60, 120 and 240 minutes (A) and kinetics of OD_{234nm} for HNE and HNEA was followed during 4 hours (B).

Supplementary Tables

Supplementary Table 1

2D molecular descriptors calculated for the 4-hydroxy-2- alkenal dérivatives

Name	Nb C=C bonds	Nb C-O bonds	Nb michael acceptors	LUMO, eV	PNSA3	PPSA3	DPSA3	WNSA3
HHE	1	1	1	-0,32	-13,85	7,95	21,79	-2,01
HNE	1	1	1	-0,35	-14,39	8,45	22,84	-2,84
HDE	1	1	1	-0,37	-14,88	8,93	23,81	-3,70
HHEA	1	5	0	1,51	-10,59	16,11	26,70	-2,17
HNEA	1	5	0	1,54	-11,10	16,59	27,69	-2,85
HDEA	1	5	0	1,56	-11,59	17,07	28,67	-3,58
HE	1	0	1	-0,27	-11,12	4,13	15,25	-1,51
NE	1	0	1	-0,25	-11,62	4,61	16,23	-2,17
DE	1	0	1	-0,25	-12,11	5,09	17,21	-2,89
HA	0	0	0	0,80	-6,66	2,43	9,09	-0,91
NA	0	0	0	0,80	-7,15	2,92	10,07	-1,35
DA	0	0	0	0,78	-7,64	3,40	11,04	-1,84

All physico-chemical parameters and 2D molecular descriptors were calculated from the web-based PreADMET application (*http://preadmet.bmdrc.org*) as described in the methods section. LUMO, lowest unoccupied molecular orbital, DPSA3, difference in atomic charge weighted surface area, PNSA3: partial negative surface area 3rd type. PPSA3, partial positive surface area 3rd type, WNSA3, surface weighted charged partial surface area 3rd type, 3nd type.

Supplementary Table 2

4-hydroxy-2- alkenal dérivative cytotoxicity predicted from QSTR models

Name	Experimental logLC50	Calculated logLC50				
		Eq. (1)	Eq.(2)[a]	Eq.(3) [a]	Eq.(4) [a]	Eq.(5) [a]
HHE	1.46	1.61	1.74	1.56	1.44	1.49
HNE	1.73	1.50	1.70	1.44	1.31	1.36
HDE	0.94	1.40	1.69	1.34	1.18	1.24
HHEA	2.11	2.30	-	-	-	-
HNEA	2.82	2.19	-	-	-	-
HDEA	2.08	2.09	-	-	-	-
HE	2.28	2.19	1.79	2.13	2.47	2.29
NE	2.53	2.08	1.81	2.03	2.34	2.17
DE	1.71	1.97	1.81	1.93	2.21	2.05
HA	2.91	3.12	2.95	3.08	2.93	3.04
NA	3.07	3.02	2.94	2.98	2.80	2.92
DA	2.74	2.91	2.92	2.87	2.67	2.80
r^2 [b]	-	0.77	0.66	0.85	0.85	0.88
P-value [c]	-	2.10^{-3}	8.10^{-3}	4.10^{-4}	4.10^{-4}	2.10^{-4}

[a] indicate that acetal dérivatives, i.e. HHEA, HNEA and HHDA were excluded for the calculation of the QSTR models.

[b] r^2 square value for the corrélation coefficient between experimental and calculated log LC50 values.

[c] significance coefficient value for the correlation between experimental and calculated log LC50 values.

Supplementary figure 1

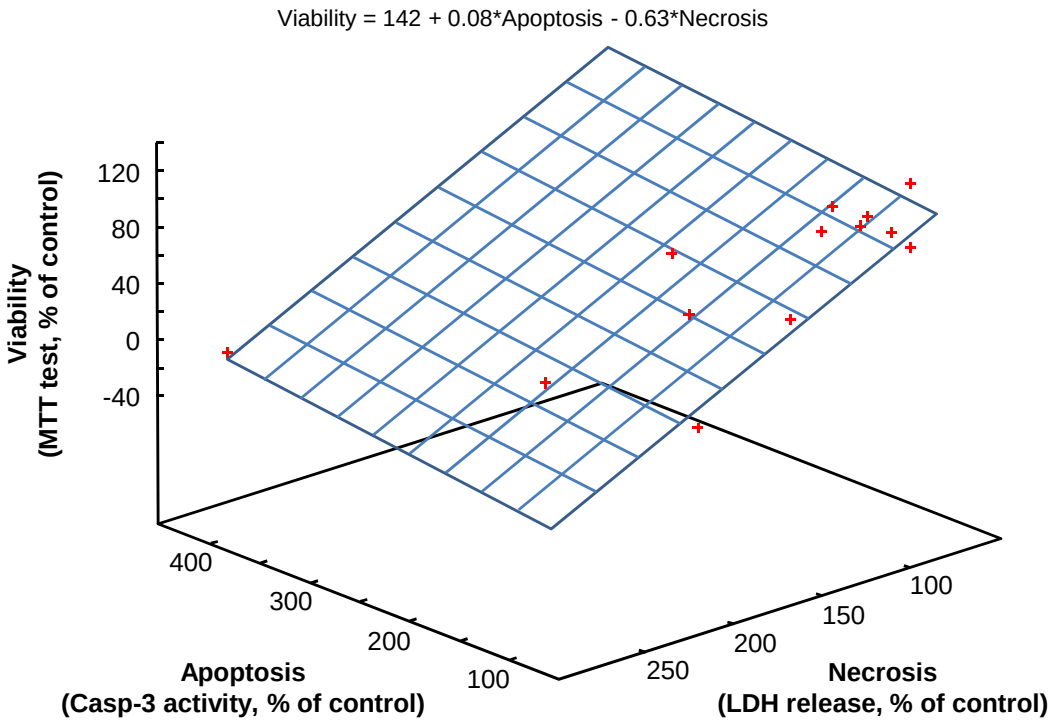

Supplementary figure 2